An Evaluation of Positioning Error Estimated by the Mesoscale Non-Hydrostatic Model

ICHIKAWA Ryuichi(richi@crl.go.jp) Kashima Space Research Center, Communications Research Laboratory

SEKO Hiromu(hseko@mri-jma.go.jp) Meteorological Research Institute, Japan Meteorological Agency

Michael BEVIS(bevis@hawaii.edu) Pacific GPS Facility, University of Hawaii

Radio Astronomy Applications Group
Kashima Space Research Center

IUGG2003, Sapporo

1. Introduction

We evaluate atmospheric parameters (equivalent zenith wet delay and linear horizontal delay gradients) derived from slant path delays obtained by ray-tracing through the non-hydrostatic numerical weather prediction model (NHM) with 1.5 km horizontal resolution [Shimada et al., 2002]. We also numerically estimate position changes caused by the horizontal variability of the water vapor by means of simulation analysis using the ray-traced slant delays. Our ultimate purpose is to establish a new method for reducing atmospheric effects on geodetic positioning. We first seek to establish the level of positioning error due to intense mesoscale and local scale phenomena. We describe preliminary results of our numerical simulation in this short report.

2. Data and Analysis scheme

The NMH which we used in our study provides temperature, humidity and pressure values at the surface and at 38 height levels (which vary between several tens meters and about 35 km), for each node in a 1.5 km by 1.5 km grid that covers Izu peninsula of the central Japan and surrounding ocean (see Figure 1). We performed ray tracing experiments for the entire grid of the NHM at one epoch of the 1200 UT 7 Mar 1997.

For each grid point we invert the simulated data set, consisting of 52 slant delays, using an isotropic and an anistropic delay model as shown in Figure 2. The isotropic model has only one parameter - the zenith wet delay (ZWD) [Niell, 1996]. The anisotropic delay model of Chen and Herring [1997] has two additional lateral gradient parameters. We compare the "true" ZWD, computed by directly integrating the wet refractivity field of the NHM, with the ZWD estimated by least squares inversion of the "observed" slant delays obtained by ray tracing. We did this using the isotropic and the anistropic delay model.

In addition we also numerically estimate atmospheric parameters and site position changes simultaneously from the ray-traced slant delays, assuming single point positioning without coordinate constraints. We consider the vector between the true position and estimated position to be the positioning error. This estimation is performed to investigate the behavior of the positioning errors generated by local atmospheric disturbances, the relation between the slant delay errors and the vertical positioning errors and so on. Our calculation scheme is illustrated in the Figure 3.

Recently, many GPS geodesists have started to weight their observations under the assumption that the standard error associated with a pointed delay measurement is proportional to cosine of the elevation angle, so to reduce the influence of low angle observations which are contaminated with multipath noise and degraded by a longer path through the atmosphere. Accordingly, we repeat our least squares analysis using this same weighting scheme and assess its impact on the relative efficacy of isotropic and anisotropic delay models.

3. Results

The ZWDs computed using ray tracing based on the vertical profile of the NHM are shown in Figure 4. Gradient vectors estimated using least squares inversion of ray-traced slant delays are also indicated (blue [elev. cut-off: 10 deg.] and red [elev. cut-off: 15 deg.] allows, respectively). At the east of the Izu peninsula ZWDs are lying in a north-south band about 10 km in width and about 50 km in length. This characteristic ZWD pattern was consistent with the observed GMS cloud images [Shimada et al., 2002]. Large gradient vectors are shown nearby the north-south ZWD band. In addition the biggest gradients occur at the northern part of the peninsula where topographic variations produce a much more complex distribution of water vapor.

We investigate the utility of the anisotropic delay model under atmospheric disturbances (of local scale) to assess its impact during GPS data processing on the estimation of geodetic station parameters. We compare the "true" position with the estimated position by least squares inversion of the ray-traced slant delays. We did this using the isotropic and the anistropic delay models. For each delay model we examined the mean bias value between true and estimated positions for each coordinate component (north, east, and vertical). We performed this analysis using both weighted and unweighted least squares inversions with 10 degrees elevation cutoff angle.

Figure 5 shows estimated positioning errors obtained at about 1500 grid points using both the isotropic (left) and anisotropic (right) atmospheric models with 10 degrees elevation cut-off. This plot represents the results obtained using unweighted least squares fits to the ray-traced slant delay data. These figures indicate that the horizontal errors are reduced by a factor of 2-3 by using the best-fitting anisotropic model at the western region of Izu peninsula. On the other hand, there is no significant improvement for reducing the horizontal errors in the northern and higher altitude regions of the peninsula and the eastern ocean of the peninsula in spite of switching from an isotropic delay model to the anisotropic delay model. In addition the band-like regions where vertical errors are large at the east of Izu peninsula correspond to those showing large ZWDs (see Figure 4). This behavior manifests the strong coupling between the vertical station coordinates and the ZWDs (at each site) in the least squares solution.

In order to be able to assess the utility of the anisotropic model at all grid points of the NHM, we have performed a statistical analysis that focuses on the reduction of positioning errors. Figure 6 shows the mean difference or bias between "true" and estimated positions for each coordinate component (i.e. the north, east, and vertical errors). This figure shows a significant reduction in the position biases is achieved when elevation angle weighting is employed. The reduction of position biases associated with adoption of an anisotropic delay model is not remarkable except for the north component.

We investigate the level of scatter of the estimated positioning errors after biases have been removed. Figure 7 shows the standard deviation of the estimated position coordinate. This figure also shows an improvement in horizontal repeatability when the elevation angle weighting is employed. This effect is the most remarkable for the east component. On the other hand, the scatter of the east component is increased when the anisotropic model is adopted. This means low elevation weighting can produce worse results in the presence of severe local disturbances of the atmosphere. The vertical component is not significantly improved (relative to a traditional treatment) by employing either elevation weighting or the anisotropic delay model.

4. Summary

By ray tracing through the output fields of the mesoscale NHM at one epoch we obtained a set of tropospheric slant delays. We invert the simulated data set, consisting of 52 slant delays using an isotropic and an anistropic delay model. We simultaneously calculate atmospheric parameters (ZWD and gradient vector) and positioning errors using this data set. We find that the positioning errors are not reduced by anisotropic mapping function, with the exception of the north-south component. Elevation weighting is more important than mapping function type for reducing horizontal errors for the present specific data set. Large horizontal and vertical positioning errors associated with topography and mountain lee wave effect are indicated. We need further investigations to understand the behavior of the atmospheric parameters and positioning error under the various topographic and meteorological regimes using the more many cases of the NHM.

References

Chen, G. and T. A. Herring, Effects of atmospheric azimuthal asymmetry on the analysis of space geodetic data, Geophys, Res. Lett., 102, 20489-20502, 1997.

Niell, A., Global mapping functions for the atmosphere delay at radio wavelength, J. Geophys. Res., 101(B2), 3227-3246, 1996.

Shimada, S., H. Seko, H. Nakamura, K. Aonashi, and Thomas A. Herring, The impact of atmospheric mountain lee waves on systematic geodetic errors observed using the Global Positioning System, Earth Planets Space, 54, 425-430, 2002.

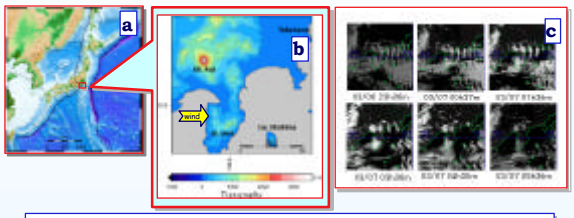

Figure 1
(a) Study area
(b) Topography of the study area
(c) Cloud images of the study area retrieved by the GMS. Atmospheric mountain waves are excited on the leeward side of the mountains[Shimada et al., 2002].

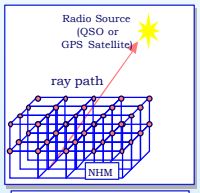

Figure 2
Schematic image of slant delay calculation using ray tracing through the NHM.

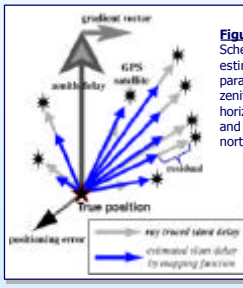

Figure 3
Schematic image showing estimations of atmospheric parameters (equivalent zenith wet delay and linear horizontal delay gradients) and station coordinates(east, north, and vertical).

Delay
-for PWV estimation-

Delay + Position
-for geodetic applications-

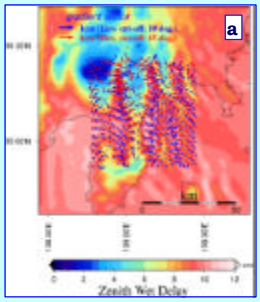

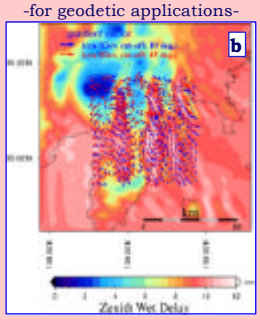

Figure 4 Zenith wet delay retrieved by the 1.5km NHM at the 1200UT of March 7, 1997. Arrows indicate gradient vectors estimated by the best-fit anisotropic model to the slant delays using ray tracing through the NHM with 10 degrees (blue) and 15 degrees (red) elevation cut-off.
(a) Atmospheric delays are only estimated.
(b) Atmospheric delays and site positions are simultaneously estimated.

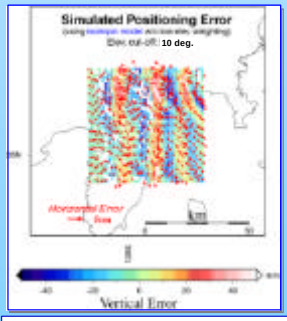

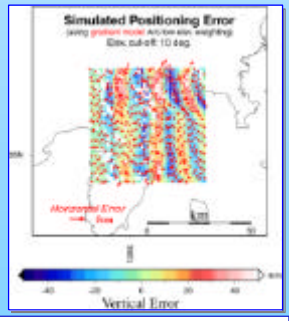

Figure 5 Estimated positioning errors (East, North, and Vertical) obtained at about 1500 grid points using both the isotropic and anisotropic atmospheric models with 10 degrees elevation cut-off.

Figure 6 Histogram of the mean bias between true and estimated positions for each coordinate component (north, east, and vertical). Estimated positions are obtained from ray-traced slant delays using isotropic and anisotropic delay models. Least squares inversions for the estimated position were performed with and without elevation angle weighting. The estimation schemes shown in the legend are as follows:

iso_unwgt isotropic model (NMF) without low elevation weighting

aiso_unwgt: anisotropic model (NMF + C&H) without low elevation weighting

iso_wgt: isotropic model (NMF) with low elevation weighting

aiso_wgt: anisotropic model (NMF + C&H) with low elevation weighting

Here, NMF and C&H denote Niell isotropic [Niell, 1996] and Chen & Herring anisotropic [Chen and Herring, 1997] mapping functions, respectively.

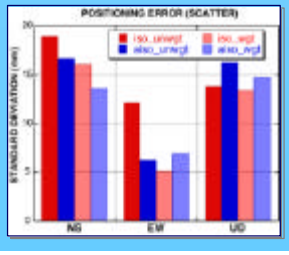

Figure 7 Standard deviation of the estimated positioning each coordinate component, pooled over all grid points. The estimation schemes are same as those considered in Figure 6.